RADIATION&APPLICATIONS
ISSN 2466-4294 (online) | rad-journal.org
Vol. 3 | Issue 3 | pp. 152–158, 2018
doi: 10.21175/RadJ.2018.03.026
Original research paper

DOSE COEFFICIENTS FOR MONOCLONAL ANTIBODIES AND ANTIBODY FRAGMENTS LABELED BY ZIRCONIUM-89*

M. V. Zhukovsky[1], Hesham M. H. Zakaly[2,3]**

[1]Institute of Industrial Ecology UB RAS, Ekaterinburg, Russia
[2]Ural Federal University, Ekaterinburg, Russia
[3]Physics Department, Faculty of Science, Al-Azhar University, Assuit Branch, Assuit, Egypt

Abstract. *The purpose was to assess the behavior of monoclonal antibodies (MAb) and their fragments labeled by ^{89}Zr after injecting them into the human body for the purpose of positron emission tomography (PET), as well as to assess absorbed doses in organs and tissues with maximum radiation exposure. The biokinetic model has been built on the base reference data about the behavior of MAb and their fragments and on the literature data on the excretion of chelate complexes from the human body. The cumulative activity of ^{89}Zr in organs and tissues per Bq of administered activity was calculated. For the most exposed organs, average absorbed doses for organs and tissues were calculated. The organs which had the highest doses, when ^{89}Zr was injected into the human body associated with intact monoclonal antibodies, are the spleen, the liver, and the heart wall. The estimated doses on these organs are 1.69, 1.48 and 1.08 mGy/MBq, respectively. When the injection associated with the fragments of monoclonal antibodies is considered, the most exposed organs are the kidneys with the doses of 0.939 mGy/MBq for F(ab')) and 0.920 mGy/MBq for F(ab')2.*

Key words: *Internal exposure, zirconium-89, monoclonal antibodies, fragments*

1. INTRODUCTION

After implementing the therapy of malignant neoplasms using antibodies in nuclear medicine, a tendency appeared for the development of tumor imaging based on target radionuclide delivery agents. Antibodies were used to transport drugs in the organism due to its specificity and affinity [1]. During the last two decades, considerable efforts have been made in developing visualization techniques using markers based on antibodies labeled with different radionuclides [2]. In the use of MAB in nuclear medicine, it is essential to have the correspondence of the physical half-life period of the radionuclide and the biological period of accumulation and half-lives of antibodies. For imaging with antibodies, radionuclides such as ^{111}In, ^{99m}Tc, ^{67}Ga, ^{86}Y, ^{64}Cu and ^{124}I [3] with half-lives time of 2.80 days; 6.0 h; 3.26 days; 14.74 h; 12.70 h; and 4.18 days, respectively [4] were used.

However, each of these radionuclides has limitations to their suitability for the resulting survey images. For example, the radionuclide ^{64}Cu was successfully used as the radioactive label of antibodies in numerous preclinical studies in rodents. However, the half-life of ^{64}Cu 12.7 h is too short for effective imaging visualization considering slow pharmacokinetics [5, 6]. The radionuclide ^{86}Y has a half-life time of 14.74 h, which is also too short to obtain high-quality images. The radionuclide ^{124}I has almost the perfect half-life time (4.18 days), and it is effectively used in PET imaging using monoclonal antibodies [7, 8]. However, the high energy of ^{124}I positrons (the maximum energy $E_{\beta max}$=2.1 Mev) and, consequently, their range in the tissue, limiting the resolution of the resulting image. The use of the radionuclide ^{99m}Tc has all the limitations specified for a single-photon emission computed tomography. In addition, it has a half-life time of 6.02 h, which is very short in terms of visualization when using antibodies [1].

Zirconium-89 is a radiotracer with suitable properties for antibody imaging. The radionuclide's half-life of 78.41 hours is long enough to match the pharmacokinetics of antibody biodistribution. It has good *in vivo* stability and low positron energy of 395 keV, thus the PET image resolution is satisfactory. In the intermediate state the short-lived radionuclide ^{89m}Y is formed. In turn, ^{89m}Y decays (T1/2=15.7 C) to the stable ^{89}Y by emitting gamma rays with energies 909 Kev [4]. The physical half-life of zirconium-89 is well suited for PET visualization based on antibodies [9]. These characteristics have stimulated the growth of interest in ^{89}Zr from a relatively little-known positron-emitting radioactive isotope to the "ideal" nuclide for the preclinical and clinical PET with the use of MAb and their fragments.

* This paper was presented at the Sixth International Conference on Radiation and Applications in Various Fields of Research (RAD 2018), Ohrid, Macedonia, 2018.

** michael@ecko.uran.ru

The use of ^{89}Zr in PET visualization requires formation of a stable chelate that is bound to a monoclonal antibody [10]. When zirconium is not bound to the chelate, it accumulates predominantly in bone tissue [11]. This is a particularly important factor in nuclear medicine. High level of accumulation of ^{89}Zr in bone tissue with the clinical diagnosis restricts the range of application containing ^{89}Zr PET agents. The various complex zirconium compounds were tested, out of which desferrioxamine (DFO) was the best and commonly used [10].

Monoclonal antibodies have been a popular means of targeting cell surface antigens during therapeutic procedures and diagnostic imaging. Monoclonal antibodies have a high affinity for their targets and many have been developed as therapies for human patients [12]. A disadvantage is that their long serum clearance times necessitate protracted imaging spanning multiple days to clear background radioactivity [13]. Monoclonal antibodies produced by the immune cells belong to the same cell clone i.e. occurred from the same cells-predecessors. In nuclear medicine, they can be used for the detection of antigens through the target delivery of antibodies labeled with radionuclides. In addition to the intact antibody molecules (molecular weight 150 kDa), fragments of antibodies to F(ab)′$_2$ and F(ab)′ [14] are used. MAb stay intact in the human body from several days to several weeks, which leads to the optimal accumulation in the tumor relative to nontumor places for 2-4 days after injection. Unlike surface MAb, MAb fragments disappear from organs and tissues much faster due to a smaller size of their molecules [14].

The dosimetry for ^{89}Zr-labeled monoclonal antibodies and fragments has been studied insufficiently. The purpose of this work is the assessment of radiation exposure of patients after the injection of ^{89}Zr-labeled monoclonal antibodies and fragments for PET visualization.

2. Materials and methods

In the practice of using radiopharmaceuticals, both intact monoclonal antibodies and their fragments are used. In the ICRP Publication 128 [14], the data on the dynamic behavior of the antibodies and fragments labeled with the radionuclides ^{99m}Tc, ^{131}I, ^{111}In, ^{123}I are presented, but the data for ^{89}Zr in publication were not found. Note that all the coefficients, which are given in Reference [14] for ^{99m}Tc, are the same for all listed radionuclides. This is due to the fact that the biological rates of radionuclide removal from an organ are determined not by the nuclide properties, but by the properties of the carrier (MAb) to which they are attached.

Radionuclides in ionic form are characterized by sufficiently high rates of transition from blood plasma to organs or tissues 10 – 100 / day^{-1} [11, 14– 17]. In the work [18] on zirconium in ionic form, the value of the rate of transition from plasma to organs and tissues is 0.69 / day^{-1}. For monoclonal antibodies, the transition speed is significantly lower. Typical biological periods of the half-life of intact MAb from the bloodstream are within the range from 10 to 200 h [19-22]. In some cases, a combination of fast and slow excretion of the drug from the bloodstream [23] is observed. Fragments of the MAb are characterized by a high rate of excretion of the drug from the bloodstream [2, 23, 25].

The objective of this study is a general assessment of radiation exposure of tissues and organs, without connection to specific monoclonal antibodies or their fragments. Therefore, according to the averaged data for calculations, the following are the values of the half-life times of the radiotracer transfer from the bloodstream to organs and tissues [19 – 22]:

- 50 h for intact MAb;
- 12h for fragments of MAb (ab)′2;
- 6 h for fragments of MAb (ab)′.

There are some common features in the behavior of antibodies. After intravenous injection, the highest activity is observed in organs with high vascular perfusion, that is, in the liver, spleen, bone marrow and kidneys [14]. For intact antibodies, there are two elimination rates. Based on this approach, a model of the radionuclide behavior in the body was developed. A biokinetic model of the behavior of ^{89}Zr, associated with intact antibodies, is shown in Fig. 1.

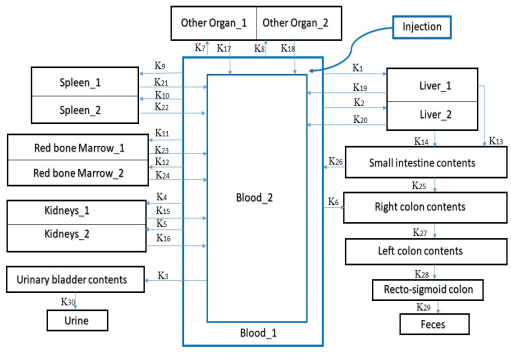

Figure 1. Biokinetic model of the behavior of ^{89}Zr, associated with intact antibodies

The compartment, from which the radionuclides transfer to organ and tissues, was marked as “Blood_1.” The nuclides were initially injected into the compartment in the form of compound-labeled intact MAb. After the absorption of the compound into the organ, the reverse excretion is associated with the metabolism of antibodies and the release of the radionuclide [14].

After the destruction of MAb due to metabolism, the behavior of released radionuclides depends on their chemical form and properties. For example, in the ICPP publication [14], the use of a biokinetic model for pertechnetate is recommended after releasing ^{99m}Tc from antibodies or their fragments. When ^{111}In is released, the biokinetic model for indium in ionic form should be used. The most used form of ^{89}Zr for labeling MAb is the chelating compounds, out of which desferrioxamine DFO or its modified form DFO* became the one commonly used [10, 26]. Zr-DFO shows good stability to demetallization, releasing less than 0.2% of the metal in the blood plasma after 24 hours [10]. The modified Zr-DFO* also demonstrated good stability and considerable decrease of ^{89}Zr

absorption in bone tissues. Since zirconium remains bound to the chelate, to describe the excretion, a model for zirconium in the ionic form [18] was not used. Instead, a model for the behavior of chelate complexes was considered. Traditionally, the chelate complexes are used to excrete plutonium from the body, and this process is more studied. The excretion of ^{89}Zr from the organs and tissues is not going to the compartment "blood-1", but to the compartment "blood-2." Note that these two compartments are not two different blood systems but the compounds with a different excretion and absorption rates for the blood, organs and tissues. The constant of excretion of the chelate complex is taken from [27, 28]. The rates of transport through the gastrointestinal tract and urine excretory system are standard and are given in Publications 100 ICRP [15]. The calculated transition rates for intact MAb, labeled with ^{89}Zr, are presented in Table 1.

Table 1. Parameters of the biokinetic model for intact MAbs labeled with ^{89}Zr

Name	Path	Transition rate, day-1
k1	Blood_1 → Liver_1	8.30E-02
k2	Blood_1 → Liver_2	8.30E-02
k3	Blood_2 → UB_Cont	5.33E+01
k4	Blood_1 → Kidneys_1	5.00E-03
k5	Blood_1 → Kidneys_2	5.00E-03
k6	Blood_1 → R_Colon	1.29E-02
k7	Blood_1 → Other_1	3.00E-02
k8	Blood_1 → Other_2	3.00E-02
k9	Blood_1 → Spleen_1	1.50E-02
k10	Blood_1 → Spleen_2	1.50E-02
k11	Blood_1→R_Marrow_1	3.33E-02
k12	Blood_1→R_Marrow_2	3.33E-02
k13	Liver_1 → SI_Cont	9.24E-04
k14	Liver_2 → SI_Cont	9.24E-04
k15	Kidneys_1 → Blood_2	6.90E-01
k16	Kidneys_2 → Blood_2	1.73E-01
k17	Other_1 → Blood_2	6.90E-01
k18	Other_2 → Blood_2	1.73E-01
k19	Liver_1 → Blood_2	6.90E-01
k20	Liver_2 → Blood_2	1.73E-01
k21	Spleen_1 → Blood_2	6.90E-01
k22	Spleen_2 → Blood_2	1.73E-01
k23	R_Marrow_1 → Blood_2	6.90E-01
k24	R_Marrow_2→Blood_2	1.73E-01
k25	SI_Cont → R_Colon	6.00E+00
k26	SI_Cont → Blood_2	3.00E-01
k27	R_Colon → L_Colon	1.80E+00
k28	L_Colon → Rectosigmoid	2.00E+00
k29	Rectosigmoid → Feces	1.00E+00
k30	UB_Cont → Urine	1.20E+01

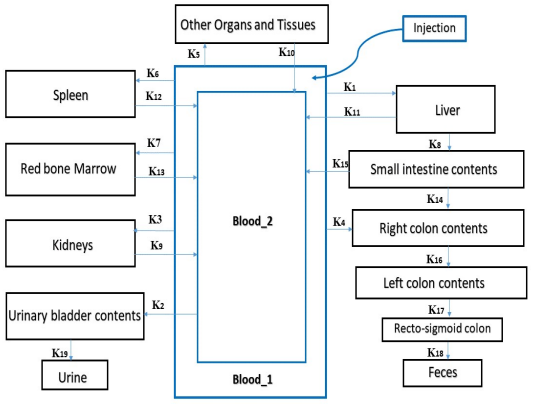

Figure 2. The biokinetic model ^{89}Zr, which is associated with the fragments MAb

Table 2. Parameters of the biokinetic model for ^{89}Zr, associated with fragments F(ab')2 and F(ab)' MAb

Name	Path	Transition rate, day^{-1}	
		F(ab')2 of MAb	F(ab') of MAb
k1	Blood_1 → Liver	4.14E-1	4.14E-1
k2	Blood_2→ UB_Cont	5.33E+1	5.33E+1
k3	Blood_1 → Kidneys	2.76E-1	2.76E-1
k4	Blood_1 → R_Colon	1.29E-2	1.29E-2
k5	Blood_1 → Other	4.69E-1	4.69E-1
k6	Blood_1 → Spleen	8.28E-2	8.28E-2
k7	Blood_1 → R_Marrow	1.38E-1	1.38E-1
k8	Liver → SI_Cont	9.24E-4	9.24E-4
k9	Kidneys → Blood_2	1.39E+0	1.39E+0
k10	Other → Blood_2	1.39E+0	1.39E+0
k11	Liver → Blood_2	1.39E+0	1.39E+0
k12	Spleen → Blood_2	1.39E+0	1.39E+0
k13	R_Marrow →Blood_2	1.39E+0	1.39E+0
k14	SI_Cont → R_Colon	6.0E+0	6.00E+0
k15	SI_Cont → Blood_2	3.00E-1	3.00E-1
k16	R_Colon → L_Colon	1.80E+0	1.80E+0
k17	L_Colon → Rectosigmoid	2.00E+0	2.00E+0
k18	Rectosigmoid → Feces	1.00E+0	1.00E+0
k19	UB_Cont → Urine	1.20E+1	1.20E+1

A simpler biokinetic model for antibody fragments is shown in Figure 2. The transition rates of the compound ^{89}Zr labeled with fragments F(ab)′2 and F(ab)′ MAb are represented in Table 2, respectively.

3. Results and Discussion

For the calculation of radionuclide dynamic in the human body, the WinAct 1.0 software package, developed at the Oak Ridge National Laboratory, and available on their website https://www.ornl.gov/crpk/software, was used [29].

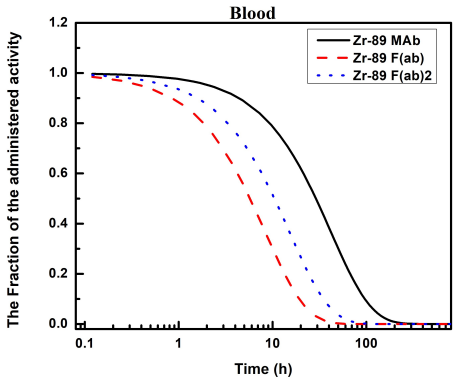

Figure 3. The dependence of the activity of radiopharmaceutical in blood on the time after intravenous injection

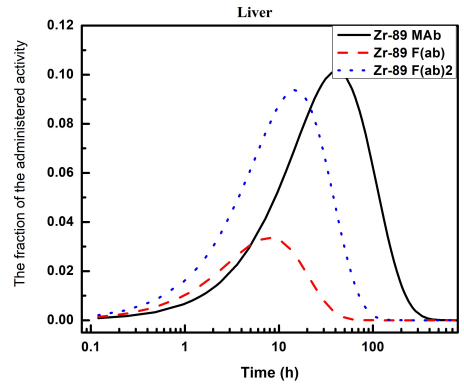

Figure 4. The dependence of the activity of radiopharmaceutical in liver on the time after intravenous injection

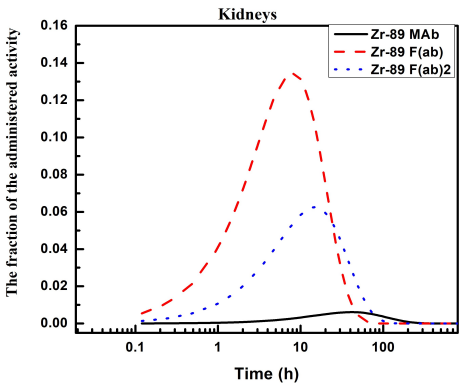

Figure 5. The dependence of the activity of radiopharmaceutical in kidneys on the time after intravenous injection

Figures 3-5 show the dependence of the activity of radiopharmaceutical in various organs on the time after intravenous injection. The figures show that the fragments of MAb labeled with ^{89}Zr are characterized by both faster accumulations in the organs and a faster excretion of the radionuclide in comparison to intact MAb. In order to assess the potential threat to the patient from exposure to radiopharmaceuticals use, the absorbed doses were calculated for the organs with the maximal accumulation of the labeled complex: the kidneys, red bone marrow, spleen and liver. Since the ^{89}Zr emits its own of gamma rays and gamma rays as a result of positron annihilation, it was also necessary to calculate the absorbed doses for the adjacent organs (the targeted organs), which are exposed by the source organ. The injection is administered directly into the blood that circulates throughout the body, and, largely, in the lungs, so the assessment of the absorbed dose from this source is required.

Additionally, the contribution to the lungs, red marrow and gonads from such source as "other organs and tissues" was assessed. The assessments showed that for the rest of the internal organs the contribution to the dose is less by one or two orders of magnitude than it is for the listed organs, so a detailed calculation of the doses for them was not performed.

Calculations were made for three types of injections: intact antibody, as well as the fragments of antibodies F (ab)'2 and F (ab)', labeled ^{89}Zr. All calculations were made of the absorbed doses administered for injection 1 activity in Bq. The data on the cumulative activity of N radionuclide ^{89}Zr in organs and tissues, normalized at 1 Bq of injection activity for intact antibody or the antibody fragments of antibodies, labeled ^{89}Zr, are presented in Table 3.

Table 3. Cumulated activity (normalized to 1 Bq introduced activity) and residence time in organs when administered to intact antibodies and their fragments labeled with ^{89}Zr.

Organ or tissue	Number of decays N (Residence time, h)		
	Intact MAb	Fragments Mab F(ab)'2	Fragments Mab
Kidneys	2.67E+03 (0.74)	9.06E+03 (2.51)	1.06E+04 (2.94)
Liver	4.42E+04 (12.3)	1.36E+04 (3.78)	2.64E+03 (0.73)
Red bone marrow	1.78E+04 (4.94)	4.53E+03 (1.26)	7.92E+02 (0.22)
Spleen	8.00E+03 (2.22)	2.72E+03 (0.75)	5.28E+02 (0.15)
Urinary bladder	2.39E+03 (0.66)	5.12E+03 (1.42)	5.97E+03 (1.66)
Blood	1.50E+05 (41.7)	5.44E+04 (15.1)	3.00E+04 (8.33)
Right Colon_cont	9.70E+02 (0.27)	3.44E+02 (0.10)	1.83E+02 (0.05)
Left Colon_cont	1.42E+03 (0.39)	5.02E+02 (0.14)	2.67E+02 (0.07)
Small intestine	6.25E+00 (~0.0)	1.92E+00 (~0.0)	3.74E-01 (~0.0)
Other organs and tissues	1.60E+04 (4.44)	1.54E+04 (4.28)	1.19E+04 (3.31)

The data on the residence time of radionuclide in organs and tissues were used as the input data to the internal dosimetry program IDAC 2.1 [29] for diagnostic nuclear medicine based on the ICRP adult reference voxel phantoms [31]. As a result, the absorbed doses to organs and tissue were estimated. The data on dose coefficients for organs and tissues are presented in Table 4.

The absorbed doses of organs and tissues depend on the form of the drug injected into the human body. At administration of ^{89}Zr associated with intact MAb considerable part of organ and tissues receive the absorbed doses from 0.5 to 1.5 mGy/MBq. When ^{89}Zr associated with intact MAb is administered into the body, the spleen, liver, heart wall and red bone marrow receive a significantly higher dose in comparison to MAb with fragments F(ab)'2 and an order of magnitude greater in comparison with fragments F(ab)'. After administration of fragments of MAb, labelled by ^{89}Zr, absorbed doses in organs considerably decreases for exception of kidneys. The patient receives the maximum dose in the kidneys, when administered ^{89}Zr, associated with fragments of MAb.

Table 4. Absorbed dose on most exposed organs and tissues when injected monoclonal antibodies and fragments, labeled with ^{89}Zr

Organ or tissue	Intact MAb, mGy/MBq	Fragments MAb F(ab)′2, mGy/MBq	Fragments MAb F(ab)′, mGy/MBq
Adipose/residual tissue	1.50E-01	7.42E-02	4.82E-02
Adrenals	9.72E-01	4.93E-01	3.33E-01
Brain	1.26E-01	5.47E-02	3.22E-02
Breast	2.36E-01	9.30E-02	4.69E-02
Colon wall	4.70E-01	2.09E-01	1.34E-01
Bone surface	4.30E-01	1.65E-01	8.94E-02
Gallbladder wall	8.66E-01	3.37E-01	1.50E-01
Heart wall	1.08E+00	4.00E-01	2.10E-01
Kidneys	8.91E-01	9.20E-01	9.39E-01
Liver	1.48E+00	5.19E-01	2.04E-01
Lung	7.43E-01	2.75E-01	1.43E-01
Muscle	1.72E-01	8.10E-02	5.13E-02
Oesophagus	6.83E-01	2.54E-01	1.30E-01
Ovaries	4.43E-01	2.26E-01	1.62E-01
Pancreas	7.90E-01	3.44E-01	2.05E-01
Prostate	1.50E-01	1.48E-01	1.44E-01
Red (active) bone marrow	1.05E+00	3.87E-01	2.05E-01
Small intestine wall	4.91E-01	2.30E-01	1.53E-01
Spleen	1.69E+00	6.35E-01	2.42E-01
Stomach wall	7.53E-01	2.99E-01	1.57E-01
Testes	1.16E-01	5.88E-02	4.02E-02
Thyroid	3.22E-01	1.25E-01	6.82E-02
Urinary bladder wall	2.84E-01	3.35E-01	3.48E-01
Uterus/cervix	1.79E-01	1.77E-01	1.68E-01
Effective dose	6.05E-01	2.52E-01	1.46E-01

In general, the calculated doses for organ and tissues for intact ^{89}Zr labelled MAb are in good agreement with the results of direct dose assessment carried out in [32] where absorbed doses were calculated using OLINDA/EXM 1.0 for 20 patients (8 women and 12 men) after injection of 75 MBq of ^{89}Zr-cmAb U36 (10 mg). The different values in red marrow doses between our work and the work [32] (1.05 vs. 0.07–0.09 mSv/MBq) are related with absence of this organ as separate compartment in calculations carried out in [32]. According to the authors, "the red marrow dose was estimated using sampled blood clearance data".

The injection activity for tumor imaging using the ^{89}Zr isotope varies from 37 to 75 MBq [22]. In this case, after the use of radiopharmaceuticals in the form of intact antibodies with an activity of 75 MBq, the absorbed dose in the spleen is 127 mGy, and in the liver 111 mGy. The maximum dose in the kidneys using the fragments F(ab)' and the same injected activity is 70.4 mGy.

4. Conclusions

1. The dynamics of behavior in the body of a radiopharmaceutical based on ^{89}Zr, labeled with antibodies, are considered, a biokinetic model is constructed. The dependences of the activity of the preparation in organs and tissues from the time of its presence in an organism are determined.

2. For the most exposed organs, the dose coefficients on the unit of the injected activity were calculated.

3. It is shown that for the intact MAb administrated ^{89}Zr, in the body, the most exposed organs are the spleen, liver, kidneys, heart wall, red marrow and lungs; when administered ^{89}Zr, bound to fragments of MAb F(ab)′2 – the kidneys, spleen, liver, heart wall and lungs; with the injection of ^{89}Zr, bound to fragments of MAb F(ab)′ – the kidneys.

4. When using radiopharmaceuticals in the form of the intact antibodies with the activity of 75 MBq, the absorbed dose in the spleen will be 127 mGy, and in the liver 111 mGy. The maximum dose to the kidneys at the same injected activity, using the fragments F(ab)′, will be 70.4 mGy.

References

1. A. M. Wu, P. D. Senter, "Arming antibodies: prospects and challenges for immunoconjugates," *Nat. Biotechnol.*, vol. 23, no. 9, pp.1137 – 1146, Sep. 2005. DOI: 10.1038/nbt1141 PMid: 16151407
2. A. M. Wu, "Engineered antibodies for molecular imaging of cancer", *Methods*, vol. 65, no. 1, pp. 139 – 147, Jan. 2014. DOI: 10.1016/j.ymeth.2013.09.015 PMid: 24091005 PMCid: PMC3947235
3. T. J. Wadas, E. H. Wong, G. R. Weisman, C. J. Anderson, "Coordinating radiometals of copper, gallium, indium, yttrium, and zirconium for PET and SPECT imaging of disease," *Chem. Rev.* vol. 110, no. 5, pp. 2858 – 2902, Apr. 2010. DOI: 10.1021/cr900325h PMid: 20415480 PMCid: PMC2874951

4. *Nuclear Decay Data for Dosimetric Calculations*, ICRP Publication 107, ICRP, Ottawa, Canada, 2008.
DOI: 10.1016/j.icrp.2008.10.004
PMid: 19285593
5. W. B. Cai et al., "Quantitative PET of EGFR expression in xenograft-bearing mice using Cu-64-labeled cetuximab, a chimeric anti-EGFR monoclonal antibody," *Eur. J. Nucl. Med. Mol. Imaging*, vol. 34, no. 6, pp. 850 – 858, Jun. 2007.
DOI: 10.1007/s00259-006-0361-6
PMid: 17262214
6. P. Paudyal et al., "Imaging and biodistribution of Her2/neu expression in non-small cell lung cancer xenografts with ^{64}Cu-labeled trastuzumab PET," *Cancer. Sci.*, vol. 101. no. 4, pp. 1045 – 1050, Apr. 2010.
DOI: 10.1111/j.1349-7006.2010.01480.x
PMid: 20219072
7. P. K. E. Borjesson et al., "Performance of Immuno-Positron Emission Tomography with Zirconium-89 Labeled Chimeric Monoclonal Antibody U36 in the Detection of Lymph Node Metastases in Head and Neck Cancer Patients," *Clin. Cancer. Res.*, vol. 12, no. 7, pp. 2133 – 2140, Apr. 2006.
DOI: 10.1158/1078-0432.CCR-05-2137
PMid: 16609026
8. I. Verel et al., "High-quality ^{124}I-labelled monoclonal antibodies for use as PET scouting agents prior to ^{131}I-radioimmunotherapy," *Eur. J. Nucl. Med. Mol. Imaging*, vol. 31, no. 12, pp. 1645 – 1652, Dec. 2004.
DOI: 10.1007/s00259-004-1632-8
PMid: 15290121
9. J. P. Holland, M. J. Williamson, J. S. Lewis, "Unconventional Nuclides for Radiopharmaceuticals," *Mol. Imaging*, vol. 9, no. 1, pp. 1 – 20, Jan. 2010.
DOI: 10.2310/7290.2010.00008
PMid: 20128994
PMCid: PMC4962336
10. W. E. Meijs, J. D. M. Herscheid, H. J. Haisma, H. M. Pinedo, "Evaluation of desferal as a bifunctional chelating agent for labeling antibodies with Zr-89," *Appl. Radiat. Isot.*, vol. 43, no. 12, pp. 1443 – 1447, Dec. 1992.
DOI: 10.1016/0883-2889(92)90170-J
11. C. R. Fletcher, "The radiological hazards of zirconium-95 and niobium-95," *Health Phys.*, vol. 16, no. 2, pp. 209 – 220, Feb. 1969.
DOI: 10.1097/00004032-196902000-00011
PMID: 5772185
12. S. M. Chiavenna, J. P. Jaworski, A. Vendrell, "State of the art in anti-cancer mAbs," *J. Biomed. Sci.*, vol. 24, no. 15, pp. 1 – 12, Feb. 2017.
DOI: 10.1186/s12929-016-0311-y
13. L. Lindenberg et al., "Dosimetry and first human experience with ^{89}Zr-panitumumab," *Am. J. Nucl. Med. Mol. Imaging*, vol. 7, no. 4, pp. 195 – 203, 2017.
PMid: 28913158
PMCid: PMC5596322
14. *Radiation Dose to Patients from radiopharmaceuticals: A Compendium of Current Information Related to Frequently Used Substances*, ICRP Publication 128, ICRP, Ottawa, Canada, 2015.
DOI: 10.1177/0146645314558019
PMid: 26069086
15. *Human Alimentary Tract Model for Radiological Protection*, ICRP Publication 100, ICRP, Ottawa, Canada, 2006.
DOI: 10.1016/j.icrp.2006.03.004
PMid: 17188183
16. R. W. Leggett, "The biokinetics of inorganic cobalt in the human body," *Sci. Total Environ.*, vol. 389, no. 2-3, pp. 259 – 269, Jan. 2008.
DOI: 10.1016/j.scitotenv.2007.08.054
PMid: 17920105
17. R. W. Leggett, "A biokinetic model for zinc for use in radiation protection," *Sci. Total Environ.*, vol. 420, pp. 1 – 12, Mar. 2012.
DOI: 10.1016/j.scitotenv.2012.01.013
PMid: 22326317
18. W. B. Li, M. Greiter, U. Oeh, C. Hoeschen, "Reliability of a new biokinetic model of zirconium in internal dosimetry: part II, parameter sensitivity analysis," *Health Phys.*, vol. 101, no. 6. pp. 677 – 692, Dec. 2011.
DOI: 10.1097/HP.0b013e318226edc0
19. J. A. Carrasquillo et al., "(124)I-huA33 Antibody PET of Colorectal Cancer," *J. Nucl. Med.*, vol. 52, no. 8, pp. 1173 – 1180, Jul. 2011.
DOI: 10.2967/jnumed.110.086165
PMid: 21764796
PMCid: PMC3394182
20. A. L. Klibanov et al., "Blood Clearance of Radiolabeled Antibody: Enhancement by Lactosamination and Treatment with Biotin-Avidin or Anti-Mouse IgG Antibodies" *J. Nucl. Med.*, vol. 29, no. 12, pp. 1951 – 1956, Dec. 1988.
PMID: 2848113
21. D. R. Mould, K. R. D. Sweeney, "The pharmacokinetics and pharmacodynamics of monoclonal antibodies – mechanistic modeling applied to drug development," *Curr. Opin. Drug Discov. Devel*, vol. 10, no. 1, pp. 84 – 96, Jan. 2007.
PMid: 17265746
22. E. C. Dijkers et al., "Biodistribution of ^{89}Zr-trastuzumab and PET Imaging of HER2-Positive Lesions in Patients With Metastatic Breast cancer," *Clin. Pharmacol. Ther.*, vol. 87, no. 5, pp. 586 – 592, May 2010.
DOI: 10.1038/clpt.2010.12
PMid: 20357763
23. I. Buchmann et al., "A comparison of the biodistribution and biokinetics of ^{99m}Tc-anti-CD66 mAb BW 250/183 and ^{99m}Tc-anti-CD45 mAb YTH 24.5 with regard to suitability for myeloablative radioimmunotherapy," *Eur. J. Nucl. Med. Mol. Imaging*, vol. 30, no. 5, pp. 667 – 673, May 2003.
DOI: 10.1007/s00259-002-1106-9
PMid: 12599012
24. C.-A. Vogel et al., "Direct comparison of a radioiodinated intact chimeric anti-CEA MAb with its F(ab')2, fragment in nude mice bearing different human colon cancer xenografts," *Br. J. Cancer*, vol. 68, no. 4, pp. 684 – 690, Oct. 1993.
DOI: 10.1038/bjc.1993.410
PMid: 8398694
PMCid: PMC1968595
25. T. Olafsen et al., "Optimizing Radiolabeled Engineered Anti-p185HER2 Antibody Fragments for in vivo Imaging," *Cancer Res.*, vol. 65, no. 13, pp. 5907 – 5916, 2005.
DOI: 10.1158/0008-5472.CAN-04-4472
PMid: 15994969
PMCid: PMC4161125
26. J. W. Stathler et al., "The Retention of ^{14}C-DTPA in Human Volunteers after Inhalation or Intravenous Injection," *Health Phys.*, vol. 44, no. 1. pp. 45 – 52, Jan. 1983.
DOI: 10.1097/00004032-198301000-00006
27. V. F. Khokhryakov et al., "Successful DTPA Therapy in the Case of 239Pu Penetration via Injured Skin Exposed to Nitric Acid," *Radiat. Prot. Dosim.*, vol, 105, no. 1-4, pp. 499 – 502, Jul. 2003.
DOI: 10.1093/oxfordjournals.rpd.a006291
PMid: 14527017
28. *WinAct version 1.0*, ORNL, Oak Ridge (TN), USA, 2002.
Retrieved from: https://www.ornl.gov/crpk/software;
Retrieved on: May 18, 2018

29. M. Andersson et al., "IDAC-Dose 2.1, an internal dosimetry program for diagnostic nuclear medicine based on the ICRP adult reference voxel phantoms," *EJNMMI Res*. vol. 7, no. 88, Nov. 2017.
DOI: 10.1186/s13550-017-0339-3

30. *Adult Reference Computational Phantoms*, ICRP Publication 110, ICRP, Ottawa, Canada, 2009.
DOI: 10.1016/j.icrp.2009.09.001
PMid: 19897132